Journal of Imaging Science and Technology® 55(4): 040502-1–040502-14, 2011.

Local Contrast Enhancement Based on Adaptive Multiscale Retinex Using Intensity Distribution of Input Image

In-Su Jang, Tae-Hyoung Lee▲, Wang-Jun Kyung, and Yeong-Ho Ha▲
School of Electronics Engineering, Kyungpook National University, Daegu 702-701, Korea
E-mail: yha@ee.knu.ac.kr

Abstract. *As the dynamic range of a digital camera is narrower than that of a real scene, the captured image requires a tone curve or contrast correction to reproduce the information in dark regions. Yet, when using a global correction method, such as histogram-based methods and gamma correction, an unintended contrast enhancement in bright regions can result. Thus, a multiscale retinex algorithm using Gaussian filters was already proposed to enhance the local contrast of a captured image using the ratio between the intensities of an arbitrary pixel in the captured image and its surrounding pixels. The intensity of the surrounding pixels is estimated using Gaussian filters and weights for each filter, and to obtain better results, these Gaussian filters and weights are adjusted in relation to the captured image. Nonetheless, this adjustment is currently a subjective process, as no method has yet been developed for optimizing the Gaussian filters and weights according to the captured image. Therefore, this article proposes local contrast enhancement based on an adaptive multiscale retinex using a Gaussian filter set adapted to the input image. First, the weight of the largest Gaussian filter is determined using the local contrast ratio from the intensity distribution of the input image. The other Gaussian filters and weights for each Gaussian filter in the multiscale retinex are then determined using a visual contrast measure and the maximum color difference of the color patches in the Macbeth color checker. The visual contrast measure is obtained based on the product of the local standard deviation and locally averaged luminance of the image. Meanwhile, to evaluate the halo artifacts generated in large uniform regions that abut to form a high contrast edge, the artifacts are evaluated based on the maximum color difference between each color of the pixels in a patch in the Macbeth color and the averaged color in CIELAB standard color space. When considering the color difference for halo artifacts, the parameters for the Gaussian filters and weights representing a higher visual contrast measure are determined using test images. In addition, to reduce the induced graying-out, the chroma of the resulting image is compensated by preserving the chroma ratio of the input image based on the maximum chroma values of the sRGB color gamut in the lightness–chroma plane. In experiments, the proposed method is shown to improve the local contrast and saturation in a natural way.*

[DOI: 10.2352/J.ImagingSci.Technol.2011.55.4.040502]

INTRODUCTION

Human vision is a complicated automatic self-adapting system that is capable of seeing over 5 orders of magnitude simultaneously and can gradually adapt to natural world scenes with a high dynamic range of over 9 orders of magnitude. Thus, human vision can concurrently perceive details in both bright and dark regions.[1,2] In contrast, current color imaging capture and display devices, such as digital cameras, cathode ray tubes (CRTs), liquid crystal displays (LCDs), plasma display panels (PDPs), and organic light-emitting diodes (OLEDs), are unable to capture and represent a dynamic range of more than 100:1. This means that the captured images suffer from poor scene detail and color reproduction in dark areas, especially in the case of a scene that contains both bright and dark areas. Nonetheless, despite the need to adjust the contrast of an image captured by a digital camera to represent the viewer's perception of the natural scene,[3–5] this remains a difficult problem, insofar as the human visual system is extremely complex and current techniques are unable to replicate it completely.

As the sensitivity of the human eye changes locally according to the position of an object and the illuminant in the scene, a spatially adaptive method is required to overcome these limitations, which has led to the recent development of the single-scale retinex model, based on the retinex theory as a model of human vision perception.[6] The single-scale retinex model utilizes the ratio of the lightness for a small central field in the region of interest to the average lightness over an extended field, where a Gaussian filter is generally used to obtain the average lightness. However, application of the single-scale retinex model introduces several problems, such as halos and graying-out, depending on the size of the Gaussian filter, which varies according to the input image.

Therefore, to solve these problems and stabilize the performance of the single-scale retinex model, a multiscale retinex algorithm was proposed by Jobson.[7–9] When using a small-size Gaussian filter, the local contrast and detail in the resulting image are enhanced, yet the artifacts are increased, and the opposite occurs with a large-size Gaussian filter. Thus, for the multiscale retinex algorithm, several images are created using the single-scale retinex algorithm with various sizes of Gaussian filter, and these images are then weighted and summed to reduce the halos and enhance the local contrast. However, the sizes and weights of the Gaussian filters in the multiscale retinex model are currently determined through subjective evaluation, as there is no optimization method. Moreover, if the need for contrast enhancement is low, usage of a multiscale

▲IS&T member.

Received Oct. 13, 2010; accepted for publication Apr. 22, 2011; published online Jul. 28, 2011
1062-3701/2011/55(4)/040502/14/$20.00.

retinex with fixed parameters can result in an unnaturally enhanced image.

Accordingly, to resolve these problems, this article proposes a color correction method using a multiscale retinex that takes account of the dominant chromaticity to improve the local contrast and color rendition. The sizes and weights of the Gaussian filter set for the multiscale retinex model are determined using a visual contrast measure (VCM) and halo measure. The visual contrast measure is obtained based on the product of the local standard deviation and locally averaged luminance of the image.[7] Meanwhile, the halo artifacts generated in large uniform regions with a high contrast edges are evaluated based on the maximum color difference between each color of the pixels in a patch in the Macbeth color checker and the averaged color in CIELAB standard color space. The parameters for the Gaussian filters and weights are then determined considering the visual contrast and halo measures. In addition, to enhance the input image adaptively, the weight of the largest Gaussian filter is determined according to the distribution of the local luminance in the input image. Thus, if the original image does not need to have its contrast enhanced, when the weight of large Gaussian filter becomes higher, the contrast of the resulting image remains similar to that of the original image. This happens as the resulting image from the single-scale retinex process using a large Gaussian filter is close to the original image.

For the remainder of this article, the following section provides a brief comparison of the single-scale retinex algorithm with a multiscale retinex. Thereafter, the proposed multiscale retinex algorithm is presented. Finally, experiments are used to compare the proposed method with the conventional multiscale retinex method.

Multiscale Retinex Model

The intensity I measured by a camera sensor at position X_O can be modeled as

$$I(X_I) = G(X_O)\int R(\lambda, X_O)L(\lambda)S(\lambda)d\lambda \tag{1}$$

where $G(X_O)$ is the scaling factor resulting from the geometry of the patch at position X_O, $R(\lambda, X_O)$ denotes the reflectance at position X_O, $L(\lambda)$ is the radiance given off by the light source, and $S(\lambda)$ describes the sensitivity of the sensors.[10]

It is assumed that the response functions of the sensors have a very narrow-band, i.e., they can be approximated by a delta function. Let λ_i with $i \in \{r,g,b\}$ be the wavelengths to which the sensors respond. Under a nonuniform illuminant, the intensity measured by the sensor can be modeled as follows:[2]

$$I_i(x,y) = G(x,y)R_i(x,y)L_i(x,y), \tag{2}$$

where $G(x,y)$ is the factor that depends on the scene geometry, $R_i(x,y)$ is the reflectance for wavelength λ_i, and $L_i(x,y)$ is the irradiance at position (x,y) for wavelength λ_i.

The image irradiance is proportional to the scene radiance, and since the viewing perspective is assumed to be a flat surface illuminated by a single light source, the scene radiance is proportional to the product of the irradiance falling on the surface and the reflectance of the surface. First, light of a single wavelength is considered. When assuming an orthographic projection, i.e., a direct correspondence between the image and surface coordinates, the image intensity at point (x,y) for a single band of the image is as follows:

$$I(x,y) = R(x,y)L(x,y), \tag{3}$$

where $R(x,y)$ is the reflectance at point (x,y) on the surface and $L(x,y)$ is the irradiance falling on point (x,y) on the surface. The reflectance and irradiance can be separated into two components by taking the logarithm of the sensor's response as follows:

$$\log I(x,y) = \log R(x,y) + \log L(x,y). \tag{4}$$

A Gaussian filter is used to estimate the illuminant component, and the reflectance is calculated based on the difference between the original image and the Gaussian-filtered image in logarithmic space as follows:

$$O_i(x,y) = \log I_i(x,y) - \log\{F(x,y) * I_i(x,y)\}, \tag{5}$$

where i indicates the RGB channel, $I_i(x,y)$ is the input image in the RGB channel for each coordinate position (x,y), $F(x,y)$ is the Gaussian filter, and the symbol "$*$" denotes the convolution operation.[6] The Gaussian filter is given as follows:

$$F(x,y) = Ke^{-(x^2+y^2)/\sigma^2} \text{ and } \iint F(x,y)dxdy = 1, \tag{6}$$

where K is the normalized constant coefficient and σ represents the standard deviation for the Gaussian function, which is very important, as the performance of a single-scale retinex depends on the standard deviation, σ, of the Gaussian filter. Figure 1 shows the results of a single-scale retinex when varying the standard deviation σ. When using a small scale, $\sigma = 30$, the image contrast was locally enhanced with halo artifacts, whereas a large scale, $\sigma = 90$, removed the chromaticity of the illuminant without changing the local contrast. Consequently, determining the appropriate scale is difficult, as the result of a particular scale also depends on the input image.

The idea of a multiscale retinex was introduced to stabilize the results of the single-scale retinex model. The halo artifacts resulting from a single-scale retinex using a Gaussian filter occur between the center of a uniform area and the edge of that area.[6] For example, the case of an input signal with a small peak and uniform area is shown in Figure 2(a). To estimate the illuminant component, the input signal is blurred by a Gaussian filter (Fig. 2(b)), the input signal is then divided by the blurred signal (Fig. 2(c)), and Fig. 2(d) shows the output signal. The small peak became higher after dividing the input image by the blurred image, whereas the

Figure 1. Images resulting from single-scale retinex for (a) σ =30, (b) σ =60, and (c) σ =90.

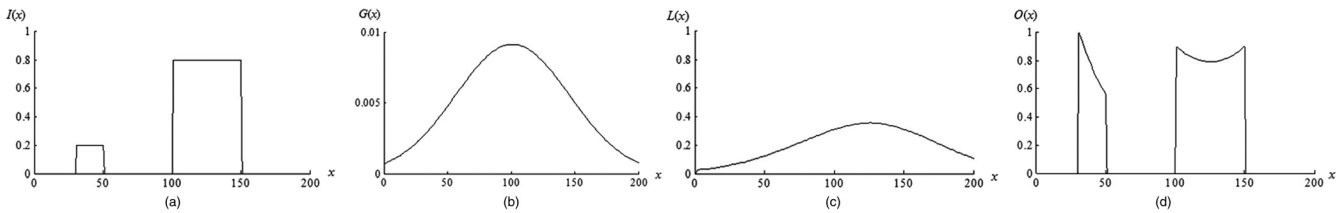

Figure 2. One-dimensional single-scaled retinex process with Gaussian filter: (a) input signal, (b) Gaussian filter, (c) filtered signal, and (d) output signal.

uniform area became concave, resulting in halo artifacts. The concavity depended on the scale of the Gaussian filter, i.e., a smaller scale produced more concavity and vice versa.

Figure 3(a) shows two Gaussian filters and Fig. 3(b) shows the output signals enhanced by the Gaussian filters and average signal of the output signals. When compared with the input signal in Fig. 2(a), the output signal with the large Gaussian filter was flatter than the other output signals instead of reducing the height of the peak. However, the concavity of the average signal was more normalized than that of the output signal with the small Gaussian filter, also the height of the peak was slightly increased.

Thus, in the multiscale retinex model,[7–9] the results for Gaussian filters with various scales are averaged with different weights using the following computation:

$$O_i(x,y) = \sum_{n=1}^{N} w_n \{\log I_i(x,y) - \log\{F_n(x,y) * I_i(x,y)\}\}, \quad (7)$$

$$F_n(x,y) = Ke^{-(x^2+y^2)/\sigma_n^2} \text{ and } \iint F_n(x,y)dxdy = 1, \quad (8)$$

where w_n represents the weight of the nth scale.

Figure 4 shows the multiscale retinex process. Generally, three Gaussian filters, small, middle, and large scale, are used to estimate the local illuminant. Images are obtained for each scale using a single-scale retinex and then averaged using a weighting factor.

Figure 5 shows the resulting images for each single-scale retinex in the multiscale retinex model. The result of the single retinex with the small-scale Gaussian filter only included detail with graying out, while the result of the single retinex with the large-scale Gaussian filter included more chromaticity information. Thus, local contrast and color rendition can be simultaneously obtained based on a weighted summation of these results.

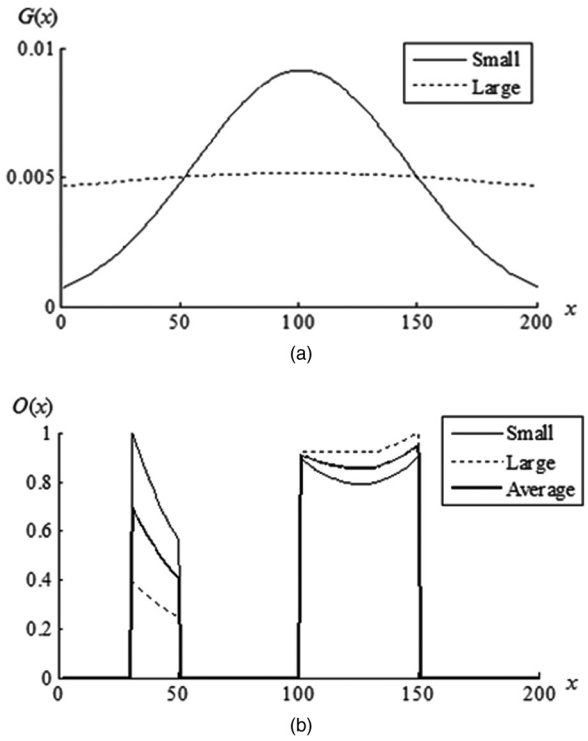

Figure 3. (a) Two Gaussian filters and (b) output signals by Gaussian filters and their average.

The multiscale retinex algorithm is very efficient for improving the detail and local contrast of shadow regions

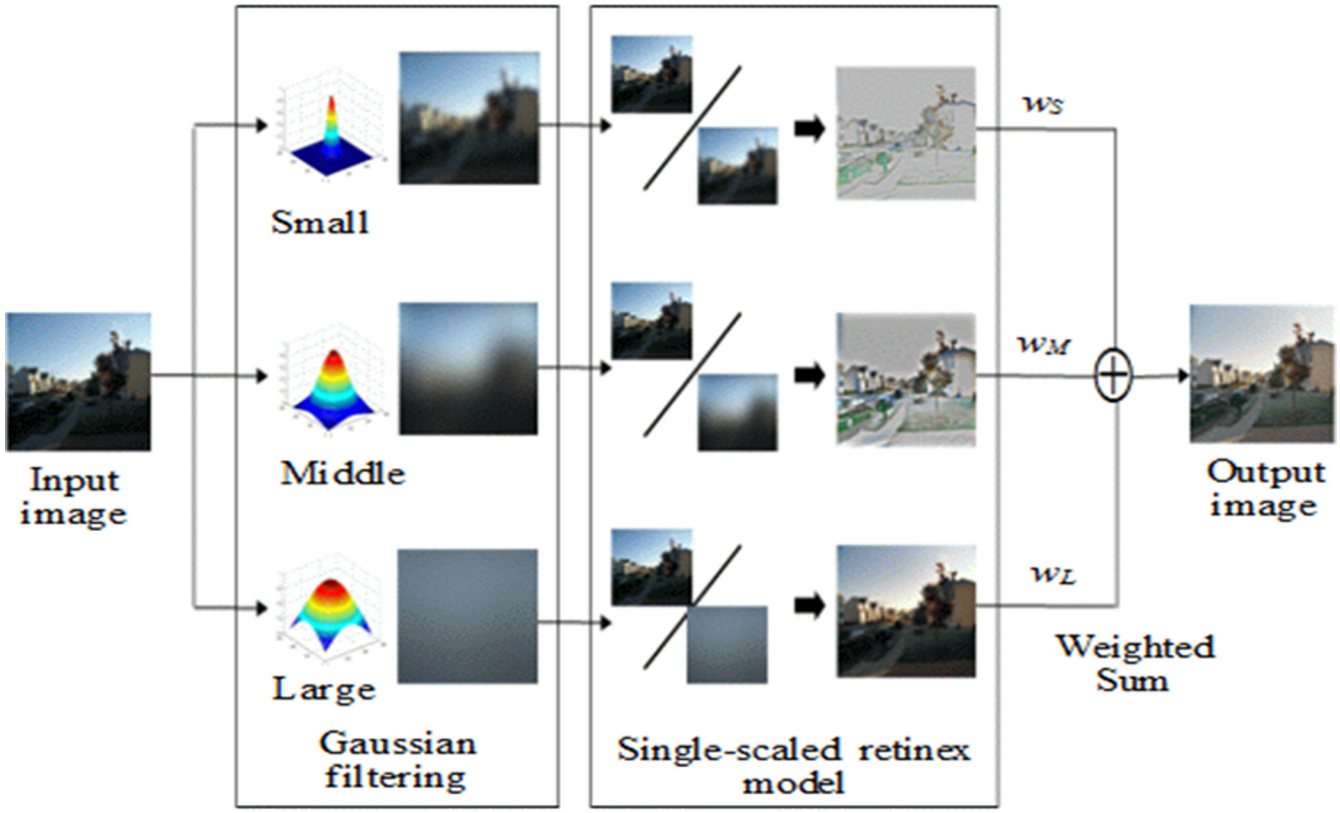

Figure 4. Multiscaled retinex process.

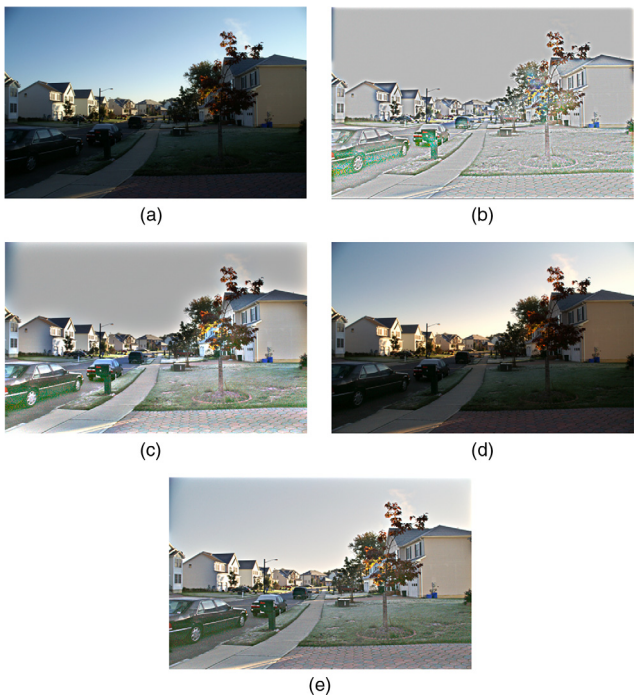

Figure 5. (a) Original image, images resulting from single-scaled retinex with (b) small scale ($\sigma = 5$), (c) middle scale ($\sigma = 20$), (d) large scale ($\sigma = 240$), and (e) images resulting from multiscaled retinex process with small, middle, and large scale.

in an image based on dividing the image by its local averaged image, regarded as the local illuminant, using a Gaussian filter. The result with a single-scale retinex algorithm depends on the scale of the Gaussian filter. The smaller the Gaussian filter, the better the local contrast, yet this also produces halo artifacts. Thus, to reduce these artifacts, the multiscale retinex algorithm uses a weighted sum of several resulting images from a single retinex with various sizes of Gaussian filter. However, selecting the appropriate Gaussian filter set and related weights remains a challenge. Even when using just two Gaussian filters, a halo artifact can be caused by the combination of the filters and their weights. The multiscale retinex process is such that, for the same input image, the resulting images for a single-scale retinex with different Gaussian filters are added in a pixel-by-pixel fashion. Each resulting image is then multiplied by different weights, causing a graying-out of the result. Plus, reducing the scale of the Gaussian filter and increasing the weight of the small Gaussian filter to enhance the local contrast can induce desaturation in the resulting image.

Visual Contrast Measure

Various sizes of Gaussian filter are used to estimate the illuminant component in the multiscale retinex model. Figure 6 shows the estimated illuminant and resulting image when using the single-scale retinex model with various sizes of Gaussian filter. In Fig. 6(b), the estimated illuminant component with a small Gaussian filter includes information on the

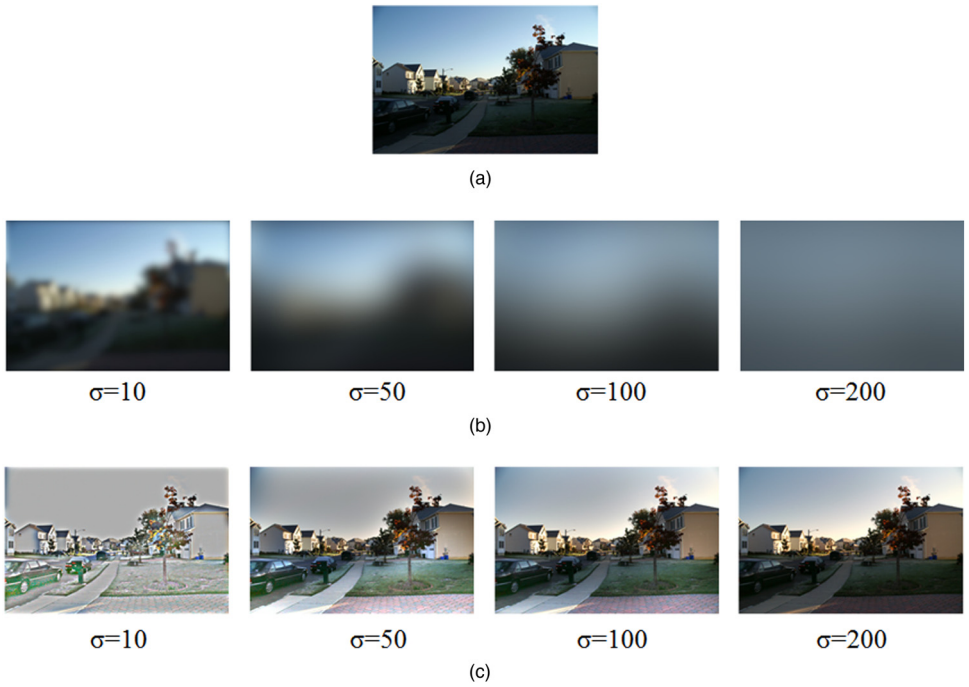

Figure 6. Contrast enhancement by various Gaussian filters: (a) input image, (b) estimated illuminant components, and (c) images resulting from single-scaled retinex.

shape of the object, whereas there is no information on the object included in the estimated illuminant component with a large Gaussian filter. When using the single-scale retinex model with a smaller Gaussian filter, the resulting image only includes details of the scene without any color information, as shown in Fig. 6(c). Meanwhile, when using a larger Gaussian filter, the contrast of the resulting image is only slightly enhanced, however, the color information is preserved from the input image, as shown in Fig. 6(a). As such, since these resulting images are summed with different weights in the multiscale retinex model, the small Gaussian filter serves to improve the local contrast, while the large Gaussian filter stabilizes the contrast enhancement by reducing the halo artifacts and preserving the color information.

Therefore, the size and weight of the large Gaussian filter are determined based on considering the local distribution of the contrast and brightness in the input image. A visual contrast measure (VCM) and halo artifact measure are then used to evaluate the resulting images from the Gaussian filters and weights.

The general idea behind the VCM is that a good visual representation usually combines a high regional visual lightness and contrast.[7] Figure 7 shows the division of an input image based on the human visual system. The best viewing angle for good color perception with the human visual system is 2°.[11] For example, in the case of a general monitor with a 1680×1050 pixel resolution, it is converted into 50 pixels based on a standard viewing distance of 45 cm. Thus, to compute the regional parameters, the input image is divided into nonoverlapping 50×50 pixel blocks.

As the regional scale is sufficiently granular to capture the visual sense of the regional brightness and contrast, the regional parameters can be used to measure the brightness and contrast. Thus, the overall lightness is measured using the image mean, which is also the ensemble measure for the regional lightness. The VCM is then computed by taking the mean of the regional standard deviations, thereby providing a gross measure of the regional contrast variations as follows:

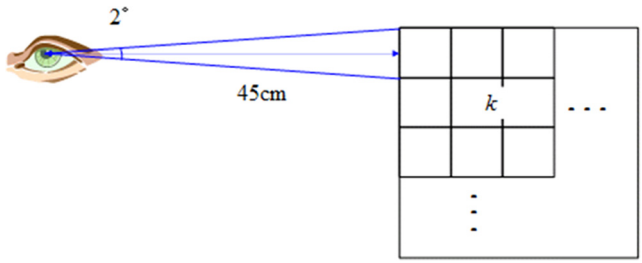

Figure 7. Division of input image based on viewing angle of human visual system.

$$V = \frac{1}{N}\sum_{k=1}^{N} m_k s_k, \tag{9}$$

where k is the index of the blocks, N is the number of blocks, m_k is the mean of the kth block, and s_k is the standard deviation of the kth block.

Halo Artifact Measure

As halo artifacts are one of the effects of using a Gaussian filter, three Gaussian filters are used in the multiscale retinex model to reduce the halo artifacts. Halo artifacts depend on the size and weight of the filter, i.e., halo artifacts appear when using a small Gaussian filter and when applying a high weight to a small Gaussian filter. Hence, to evaluate the halo

Figure 8. Macbeth color checker image for evaluation of halo artifacts.

artifacts, Macbeth color checker images were used, as shown in Figure 8. Halo artifacts occur between the center of a uniform area and the edge of that area. The Macbeth color checker also exhibits this distribution, a uniform area inside a patch and a black edge between patches. The halo artifacts are evaluated based on the maximum color difference between each color of the pixels in a patch and the averaged color in CIELAB standard color space. Assuming that the color space is standard sRGB color space, the RGB values are converted into CIEXYZ stimulus space using a 3×3 conversion matrix for standard sRGB color space as follows:[11]

$$\begin{bmatrix} X \\ Y \\ Z \end{bmatrix} = \begin{bmatrix} 0.4124 & 0.3576 & 0.1805 \\ 0.2126 & 0.7152 & 0.0722 \\ 0.0193 & 0.1192 & 0.9505 \end{bmatrix} \begin{bmatrix} R \\ G \\ B \end{bmatrix} \tag{10}$$

The XYZ values are then reconverted to CIELAB values as follows:

$$\begin{aligned} L^* &= 116\left[f\left(\frac{Y}{Y_n}\right) - \frac{16}{116}\right] \\ a^* &= 500\left[f\left(\frac{X}{X_n}\right) - f\left(\frac{Y}{Y_n}\right)\right] \\ b^* &= 200\left[f\left(\frac{Y}{Y_n}\right) - f\left(\frac{Z}{Z_n}\right)\right] \end{aligned} \tag{11}$$

$$\text{where } f(s)\begin{cases} = s^{1/3} & \text{s} > 0.008856 \\ = 7.787\ s + 16/116 & \text{otherwise,} \end{cases}$$

where X_n, Y_n, and Z_n represent the CIEXYZ values for the D65 illuminant. To evaluate the halo artifacts, the maximum color difference corresponding to each patch in the Macbeth color checker is computed as follows:

$$h_k = \max\left(\sqrt{(L^*_{m,k} - L^*_k(x,y))^2 + (a^*_{m,k} - a^*_k(x,y))^2 + (b^*_{m,k} - b^*_k(x,y))^2}\right), \tag{12}$$

where k is the index of the patch, $L^*_{m,k}$, $a^*_{m,k}$, and $b^*_{m,k}$ represent the mean of the color in the k'th patch, and $L^*_k(x,y)$, $a^*_k(x,y)$, and $b^*_k(x,y)$ represent the color at the (x,y) position in the k'th patch. Finally, the overall halo artifact measure is obtained based on the averaged maximum color differences for each patch as follows:

$$H = \frac{1}{N}\sum_{k=1}^{N} h_k, \tag{13}$$

where N indicates the number of patches in the Macbeth color checker image. As human vision cannot perceive a color difference under 3 in CIELAB color space,[12] the only Gaussian filters and weights considered had an averaged maximum color difference under 3.

Relative Local Contrast Measure

If the sizes of the Gaussian filters in the multiscale retinex model are selected only to enhance the local contrast and reduce the halo artifacts without considering the luminance and contrast distribution of the input image, this can over enhance the contrast, resulting in an unnatural image. Namely, the increase of the local contrast should be controlled according to the input image to reduce unnecessary contrast enhancement. If the input image is dark overall and the details of the objects in the dark region are not distinguished, the local contrast needs to be increased. However, when an image is captured under a relatively uniform illuminant, the local contrast should only be slightly increased.

Thus, to determine the condition of the input image, a normalized standard deviation of the local luminance based on the average luminance of the image is used as follows:

$$P = 1 - \frac{1}{\overline{m}}\sqrt{\frac{1}{N}\sum_{k=1}^{N}(m_k - \overline{m})^2}, \tag{14}$$

where k is the index of divided images, m_k represents average luminance of the k'th subimage, N is the number of subimages, and $\bar{m}$ indicates the average luminance of the input image. The normalized standard deviation of the local luminance is then reversed by subtracting from 1. Therefore, in the case of a low luminance and a high difference for the local luminance, the normalized standard deviation of the local luminance, P, is close to 0, and large in the opposite case.

Figure 9 shows the computed normalized standard deviation of the local luminance for six input images. When increasing the number of subimages, the local contrast and brightness of the image was increased, thereby reducing the necessity of contrast enhancement. Similarly, the computed P value also increased. Thus, in the multiscale retinex model, the P value is used as the weight for the large Gaussian filter to control the contrast enhancement. As such, if the standard deviation of the local luminance is high, the weight of the large Gaussian filter is

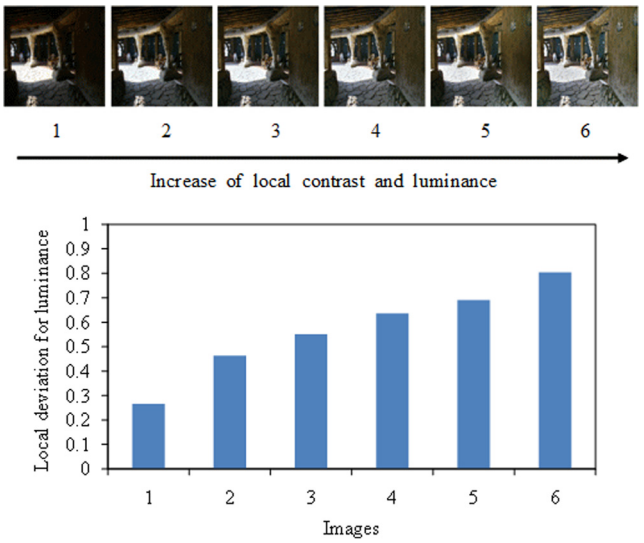

Figure 9. Normalized standard deviation of local luminance by average luminance.

increased to reduce the local contrast enhancement, and vice versa in the opposite case.

Determination of Number of Gaussian Filters Used in Multiscale Retinex

Before discussing the weights and size of the Gaussian filters, the number of Gaussian filters used in the multiscale retinex model was determined. Figure 10 shows the test images used to investigate the image changes when using a multiscale retinex with various number, size, and weight combinations of Gaussian filters. Using these ten test images, the VCM value was computed for the resulting images when varying the Gaussian filter combination. In Figure 11(a), when using two Gaussian filters, the VCM value slowly decreased when increasing the size of the small Gaussian filter. In Fig. 11(b), when using three Gaussian filters, the overall VCM values were higher than the VCM values in Fig. 11(a), plus the variation when changing the combination of Gaussian filters was also larger. In Fig. 11(c), when using four Gaussian filters, the VCM value was similar to that in Fig. 11(b), yet the variation was smaller. Finally, in Fig. 11(d), when using five Gaussian filters, the variation was smaller than that when using four Gaussian filters.

Figure 12 shows the maximum VCM for the ten test images according to the number of Gaussian filters. The case of two Gaussian filters produced the lowest VCM values, while the case of three Gaussian filters produced the highest VCM values. Therefore, even though the variation of the VCM with three Gaussian filters was larger than the variation with four and five Gaussian filters, three Gaussian filters are used for the proposed method, as the computational cost of additional Gaussian filters involves an unreasonable processing time.

Size Constraints for Gaussian Filters Used in Multiscale Retinex

Figure 13 shows the VCM evaluation results for the test images when varying the size of the small Gaussian filter. The size of the Gaussian filter is normalized according to the size of the input image. When using a Gaussian filter smaller than about 0.2, the VCM changed sharply, however, when using a Gaussian filter larger than 0.5, the VCM gradually converged to a specific value. Thus, the small Gaussian filter needed to be smaller than 0.2 to enhance the contrast.

Meanwhile, Figure 14 shows the variation of the VCM according to the size of the large Gaussian filter when using the multiscale retinex model with three Gaussian filters. For several combinations of small and middle Gaussian filters, the variation of the VCM according to the size of the large Gaussian filter was only slight. Thus, when the original image only requires minimal contrast enhancement, determining the size and weight of the large Gaussian filter is more related to reducing the halo artifacts and maintaining the color and contrast of the original image, rather than enhancing the contrast.

Figure 15 shows the averaged maximum color differences for the single-scale retinex model when varying the size of the Gaussian filter. The color difference was found to be inversely proportional to the halo artifact measure. When using a Gaussian filter smaller than 0.3 compared to the size of the input image, the color difference was more than 3, resulting in halo artifacts. In contrast, when using a Gaussian filter larger than 0.5, the color difference was smaller than 1 and converged to a minimum value over 0.8. Therefore, when considering the VCM and halo artifacts, the size of the large Gaussian filter needs to be larger than 0.8, while the size of the middle Gaussian filter needs to be constrained under 0.2 when considering the VCM.

Weight Constraints for Gaussian Filters Used in Multiscale Retinex

When determining the weight of the large Gaussian filter, halo artifacts also need to be considered, as a large Gaussian filter can play a significant role in reducing the halo artifacts with the multiscale retinex model. Figure 16 shows the averaged maximum color difference for the patches in a Macbeth color checker image as a measure of the halo artifacts. When the weight of the large Gaussian filter was lower than 0.5, the color difference was more than 3, resulting in halo artifacts. Therefore, the weight of the large Gaussian filter needs to be higher than the weights of the other two. In addition, the previously mentioned local contrast measure should be also considered to reduce unnecessary contrast enhancement.

Consequently, when using the multiscale retinex model with two Gaussian filters, the weight of the large Gaussian filter needs to be higher than that of the small Gaussian filter. Hence, in order to reduce the halo artifacts, the weight is limited to a P value ranging from 0.5 to 1 as follows:

$$w_L = \frac{P}{2} + 0.5. \tag{15}$$

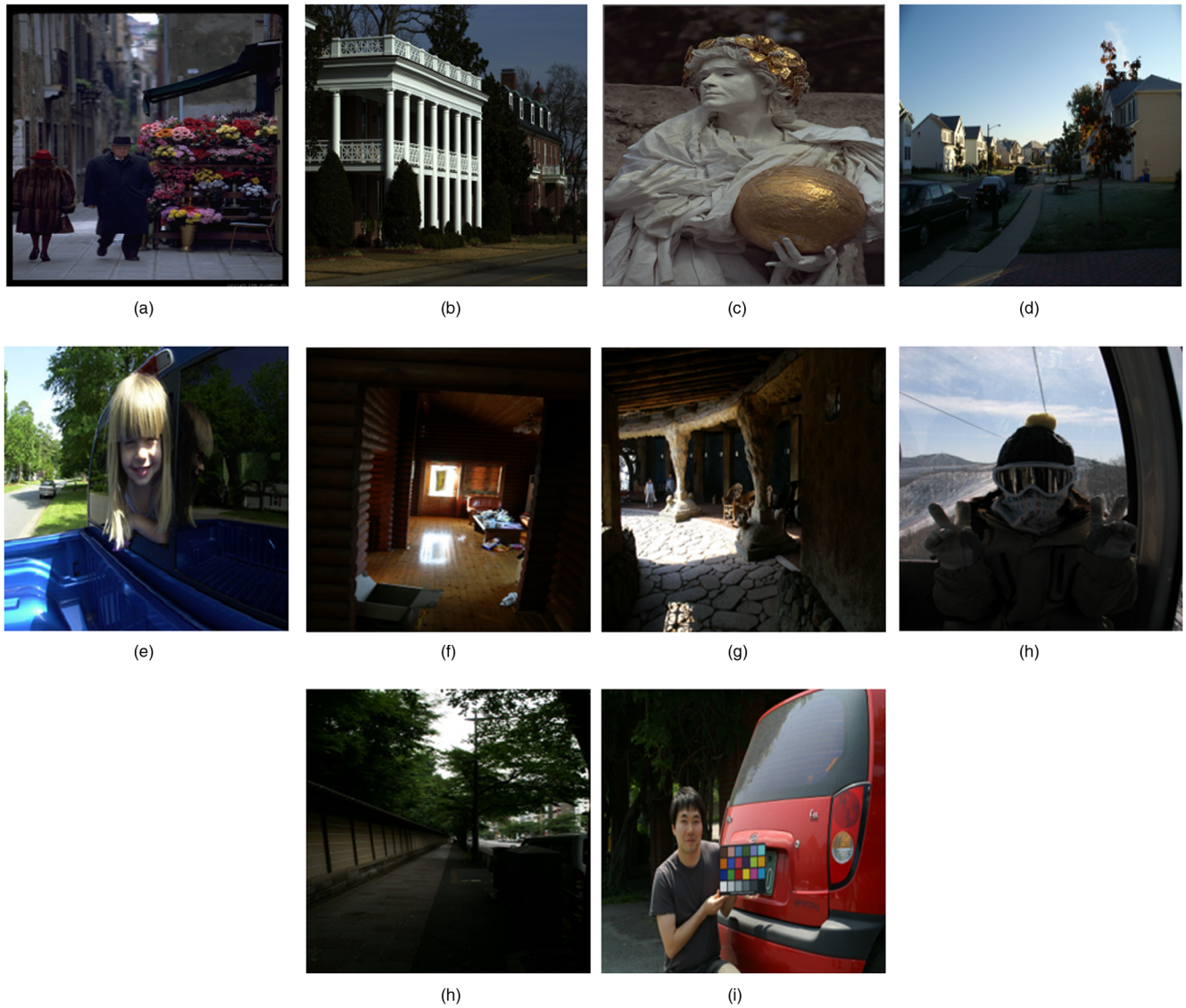

Figure 10. Test images for evaluation using VCM (a) flower, (b) mansion, (c) statue, (d) street, (e) blue car, (f) cabin, (g) cave, (h) lift, (i) road, and (j) red car.

When using the multiscale retinex model with n Gaussian filters, the limitation becomes as follows:

$$w_L = \frac{(n-1)P+1}{n}, \tag{16}$$

where n indicates the number of Gaussian filters used by the multiscale retinex model.

As a result, the size of the large Gaussian filter needs to be higher than 0.8 to reduce the halo artifacts and preserve the color information of the input image. In addition, the weight of the large Gaussian filter is determined according to the local luminance distribution of the input image. Meanwhile, the sizes of the other filters and their respective weights are determined based on the VCM and halo artifacts by changing the combination of sizes and weights. Thus, the VCM values were computed for the resulting images when using various Gaussian filter combinations with the multiscale retinex model. Among the combinations with a color difference under 3, the combination producing the largest VCM was then selected.

Selecting Size and Weight Combination of Gaussian Filters Used in Multiscale Retinex

To eliminate the halo artifacts related to each size and weight combination of Gaussian filters, the color difference was computed using a Macbeth color checker image. First, the weights were sampled based on an interval of 0.1. As regards the weight combinations, a weight of more than 0.3 was always used for the large size filter to reduce the halo artifacts, while the weights for the small and middle size filters were never the same. As a result, nine weight combinations were considered: W1=(0.333, 0.333, 0.333), W2=(0.1, 0.4, 0.5), W3=(0.4, 0.1, 0.5), W4=(0.2, 0.3, 0.5), W5=(0.3, 0.2, 0.5), W6=(0.1, 0.3, 0.6), W7=(0.3, 0.1, 0.6), W8=(0.1, 0.2, 0.7), and W9=(0.2, 0.1,

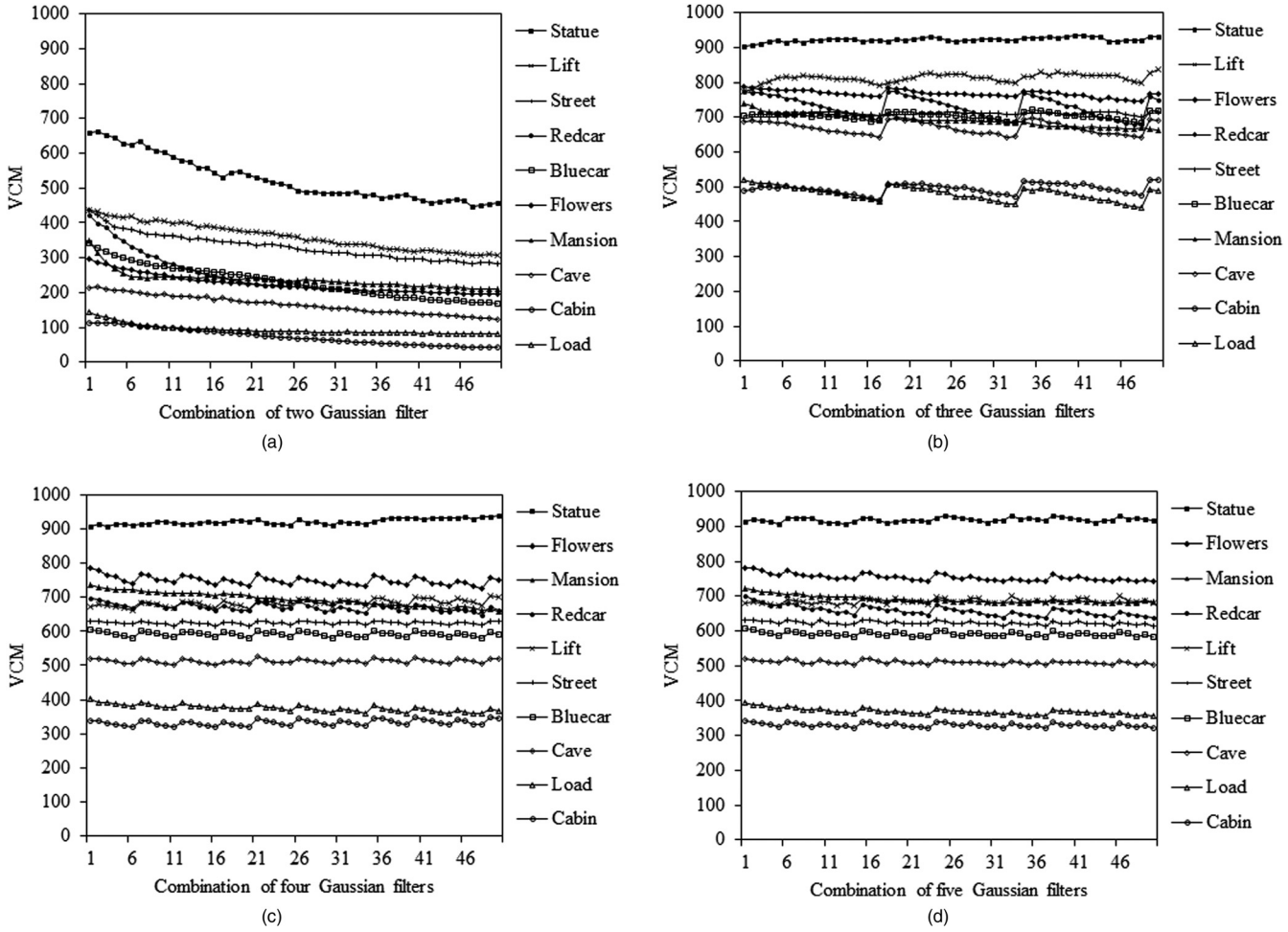

Figure 11. Variation of VCM by the number of Gaussian filters: (a) two Gaussian filters, (b) three Gaussian filters, (c) four Gaussian filters, and (d) five Gaussian filters.

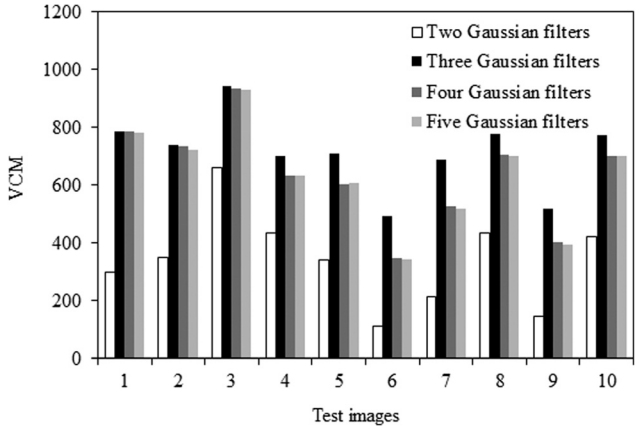

Figure 12. Maximum VCM by the number of Gaussian filter.

0.7), where W1 is the weight combination proposed by Jobson.[7]

Figure 17 shows the averaged maximum color difference for each weight combination. The W1 and W2 combinations produced an averaged maximum color difference over 3. As the weight of the large Gaussian filter became higher, the averaged maximum color difference became lower. Thus, only those combinations with a color difference under 3 were initially selected to reduce the halo artifacts. When varying the sizes and weights of the Gaussian filters under the previously mentioned constraints, the VCMs were then computed to find the optimized parameter set. Finally, the parameter set related to the maximum VCM value was selected.

Chroma Compensation

The saturation of the resulting image is lower than that of the input image, as the resulting image from a single retinex using a small-scale Gaussian filter has a very low saturation. A method for reproducing the chroma and lightness in an enhanced image was recently proposed,[7,9] where the color ratios between adjacent pixels are preserved to reproduce more original-like images. However, while this approach may be the best solution for the problem of color representation generated in an enhanced or mapped image, as preserving the ratio minimizes the color changes resulting from clipping or compression, this process is very

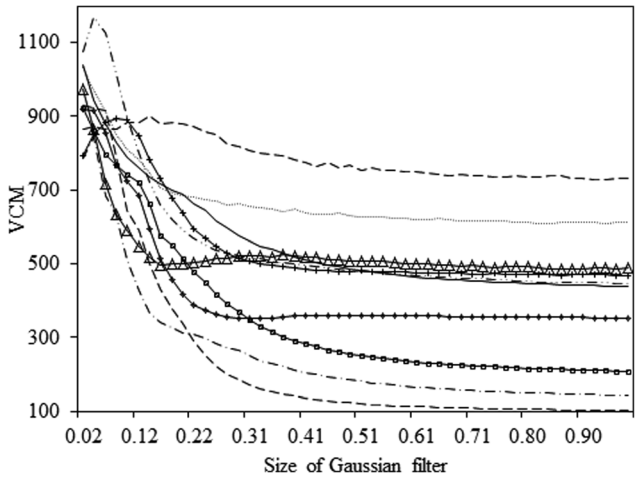

Figure 13. Computed VCM values for test images, varying scale of Gaussian filter.

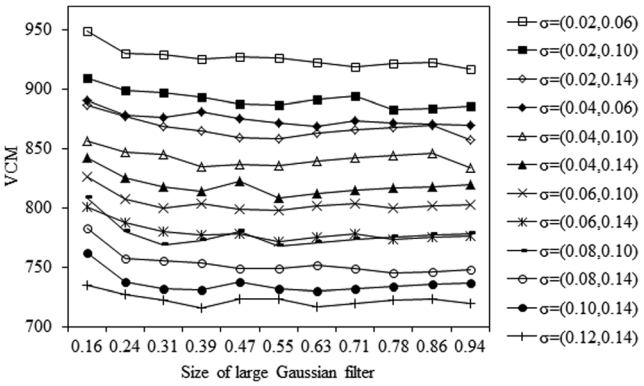

Figure 14. VCM by varying scale of large Gaussian filter.

complicated and has a high computational cost, making it hard to apply real images.

Therefore, chroma compensation is proposed using the relative chroma ratio of the input image based on the standard sRGB color gamut in CIELAB color space. The chroma value is adjusted to reduce the difference between the chroma ratio of the input image and resulting image using the proposed multiscale retinex model.

As standard sRGB color space is generally used as the image color space, the sRGB color space is converted into CIELAB color space using Eqs. (10) and (11). Since L^* represents the lightness, the chroma and hue can be computed as follows:

$$C^* = \sqrt{a^{*2} + b^{*2}} \quad \text{and} \quad H^* = \tan^{-1}\left(\frac{b^*}{a^*}\right), \tag{17}$$

where C^* is the chroma and H^* is the hue in CIELAB color space.[11] Thus, all the colors in sRGB color space are represented in CIELAB color space, as shown in Figure 18. The sRGB color gamut means the boundary of sRGB colors in CIELAB color space. Thus, the relative chroma ratio can be computed as follows:

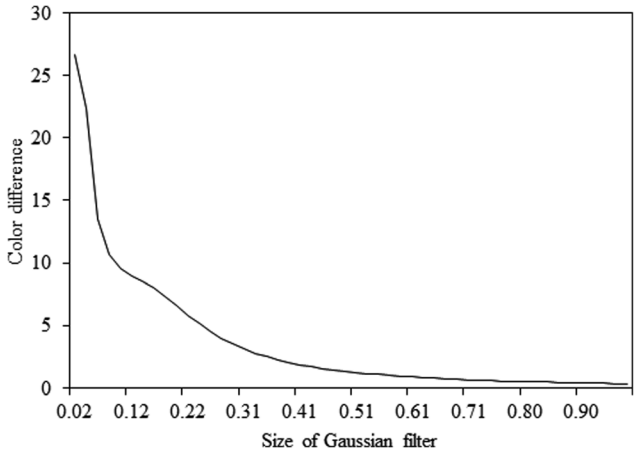

Figure 15. Averaged maximum color difference for images resulting from single-scaled retinex model, varying scale of Gaussian filter.

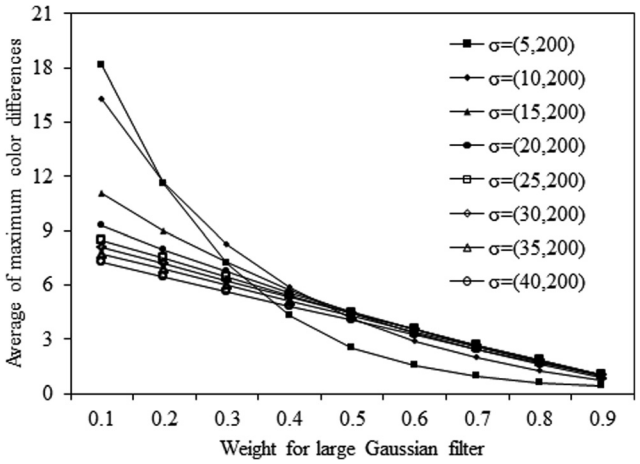

Figure 16. Halo artifacts for varying the weight of the large Gaussian filter.

$$p(x, y) = C(x, y)/C_{L,\max}, \tag{18}$$

where $C_{L,\max}$ represents the maximum chroma value in the sRGB color gamut corresponding to the lightness of the chroma, C, at position (x,y) in the same hue plane, i.e., the chroma value is normalized using the maximum value from the sRGB color gamut in CIELAB color space.

The saturation of the resulting image from a multiscale retinex is also lower than the saturation of the input image due to the averaging of the resulting images from a single-scale retinex. If the lightness of a natural scene is increased, the saturation of the natural scene is also increased simultaneously. Plus, since enhancing the contrast increases the lightness in dark regions in an image, the chroma should also be increased according to the increased lightness. However, correcting the chroma value by a simple gain can cause an unnatural color rendition due to oversaturation.

Figure 19 shows the proposed chroma compensation process. First, the maximum chroma of the sRGB color

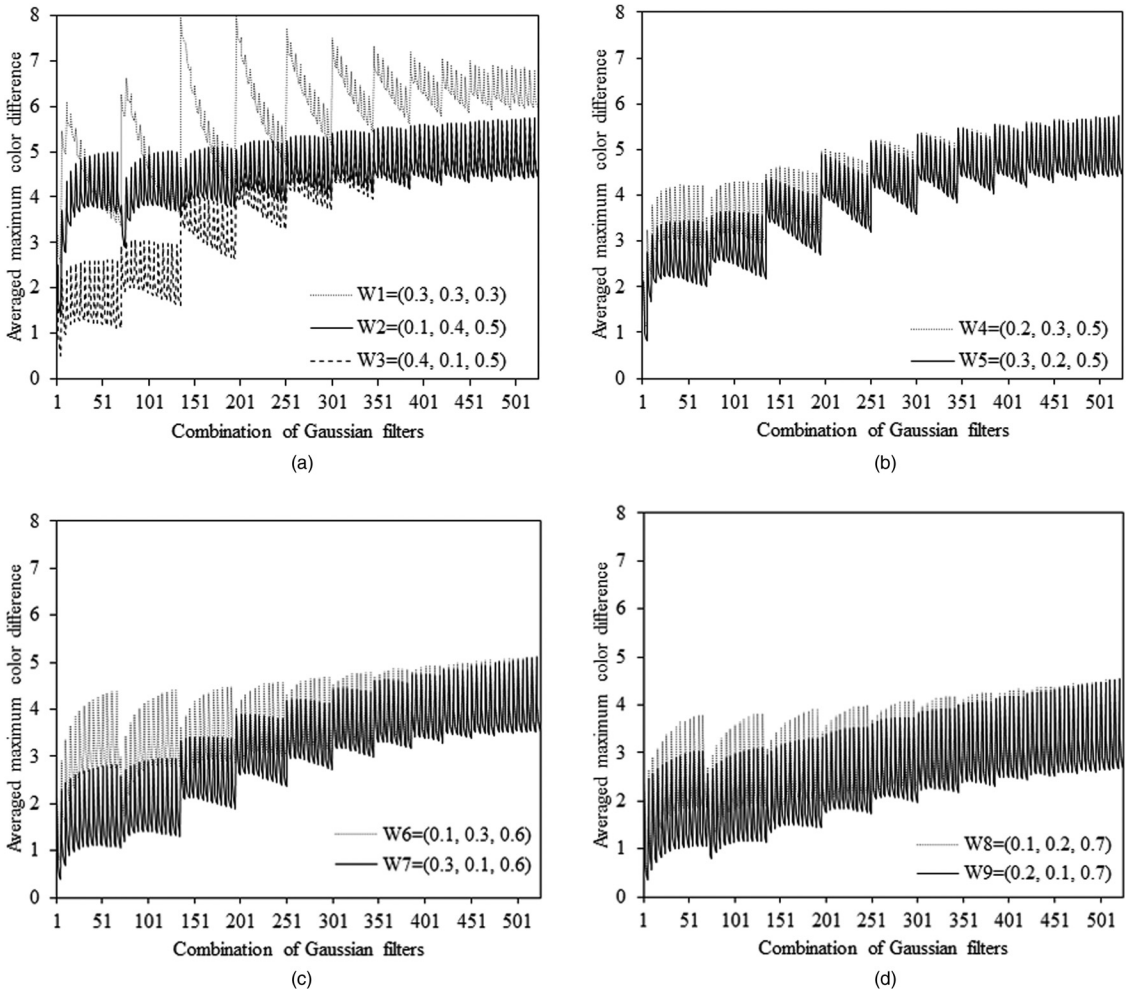

Figure 17. Averaged maximum color difference for combination of weights and Gaussian filters (a) *W*1, *W*2, and *W*3, (b) *W*4 and *W*5, (c) *W*6 and *W*7, (d) *W*8 and *W*9.

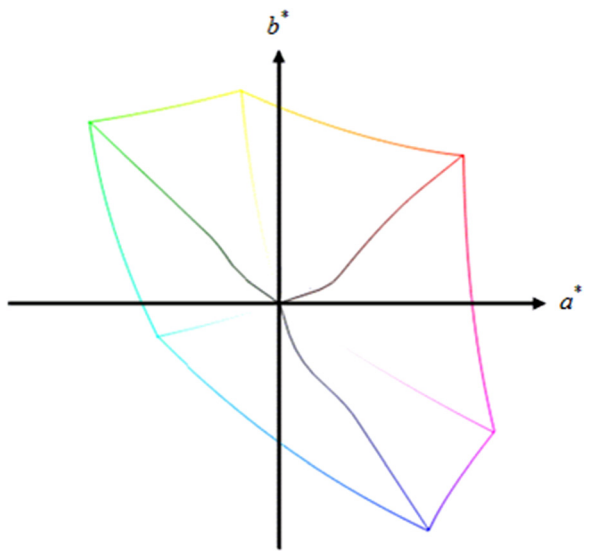

Figure 18. sRGB color gamut in CIELAB color space.

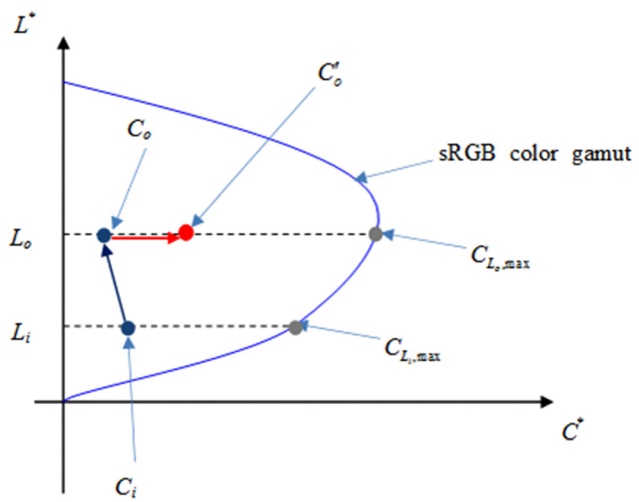

Figure 19. Chroma compensation.

Figure 20. (a) Bedroom image, and images resulting from (b) conventional multiscaled retinex, (c) proposed color correction, and (d) proposed color correction and chroma compensation.

Figure 21. (a) Veranda image, and images resulting from (b) conventional multiscaled retinex, (c) proposed color correction, and (d) proposed color correction and chroma compensation.

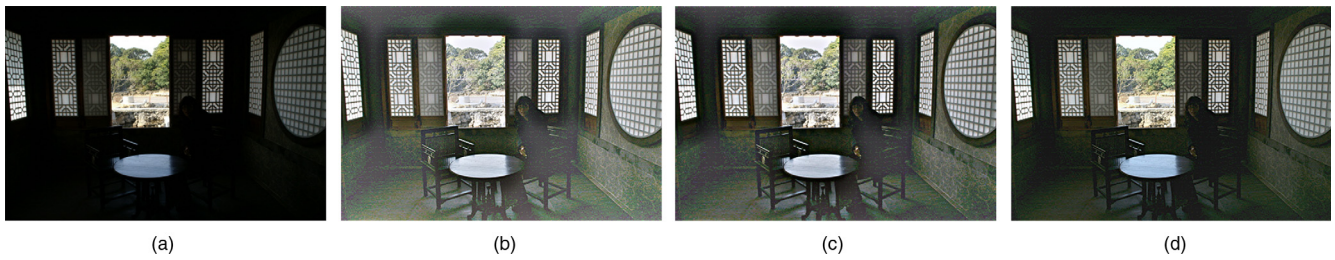

Figure 22. (a) Interior image, and images resulting from (b) conventional multiscaled retinex, (c) proposed color correction, and (d) proposed color correction and chroma compensation.

gamut is obtained according to the lightness and chroma of the input image in the same hue plane. The chroma of the resulting image from the proposed multiscale retinex is then corrected by preserving the relative chroma ratio of the input image as follows:

$$C'_o(x,y) = \frac{C_{L_o,\max}(x,y)}{C_{L_i,\max}(x,y)} \times C_i(x,y), \qquad (19)$$

where $C_{Lo,\max}$ represents the maximum chroma value corresponding to the lightness, L_o, and $C_{Li,\max}$ represents the maximum chroma value corresponding to the lightness, L_i.

EXPERIMENTS AND EVALUATION

Figures 20, 21, and 22 show the original and resulting images when using the conventional multiscale retinex with the parameter set proposed by Wang,[4] the conventional multiscale retinex with the parameter set proposed by Rahman,[7] and the proposed method. In the original image, Fig. 20(a), with the exception of the window and part of the room, no detail can be distinguished. In contrast, in Fig. 20(b), the image resulting from Wang's method, all the details can be recognized, yet noise appears on the log wall due to over-enhancement of the contrast. Also, the color of the curtain and bed is faded with respect to the original image. Similarly, in Fig. 20(c), the image resulting from Rahman's method, the saturation is a little better than that in Fig. 20(b), yet noise is still a problem. In Fig. 20(d), the image resulting from the proposed method, the color is more similar to that in the original image, the enhanced local contrast is maintained, and there is no insurgence of noise.

In Fig. 21, the color distribution is concentrated on the color beige and no noise appears due to the wide dynamic range. Thus, in Figs. 21(b) and 21(c), the color of the living room is better represented, yet halo artifacts appear on the wall above the door. However, in Fig. 21(d), there are no halo artifacts, although the local contrast enhancement is less effective. Moreover, the colors of the veranda floor (bluish) and lamp (yellowish) are better preserved.

In Fig. 22, the interior is darker than the outdoors and is quite noisy. Thus, in Figs. 22(b) and 22(c), the noise and halo artifacts are extremely intrusive, although the inner

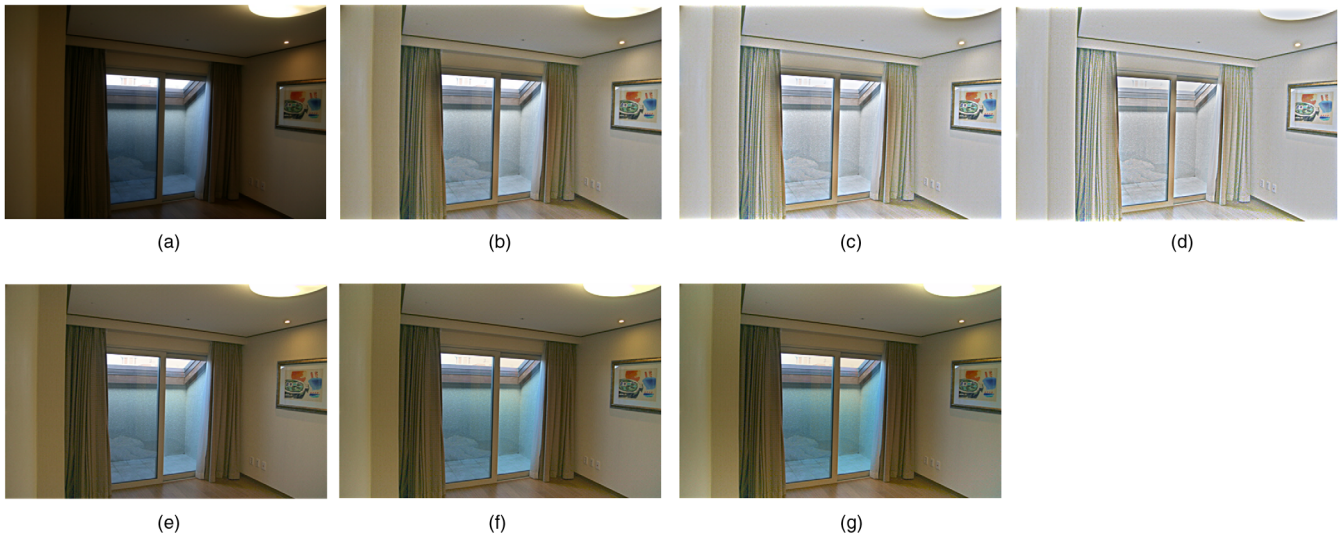

Figure 23. (a) Window image, and images resulting from application of conventional multiscaled retinex model (b) once, (c) twice, and (d) three times, and applying proposed method (e) once, (f) twice, and (g) three times.

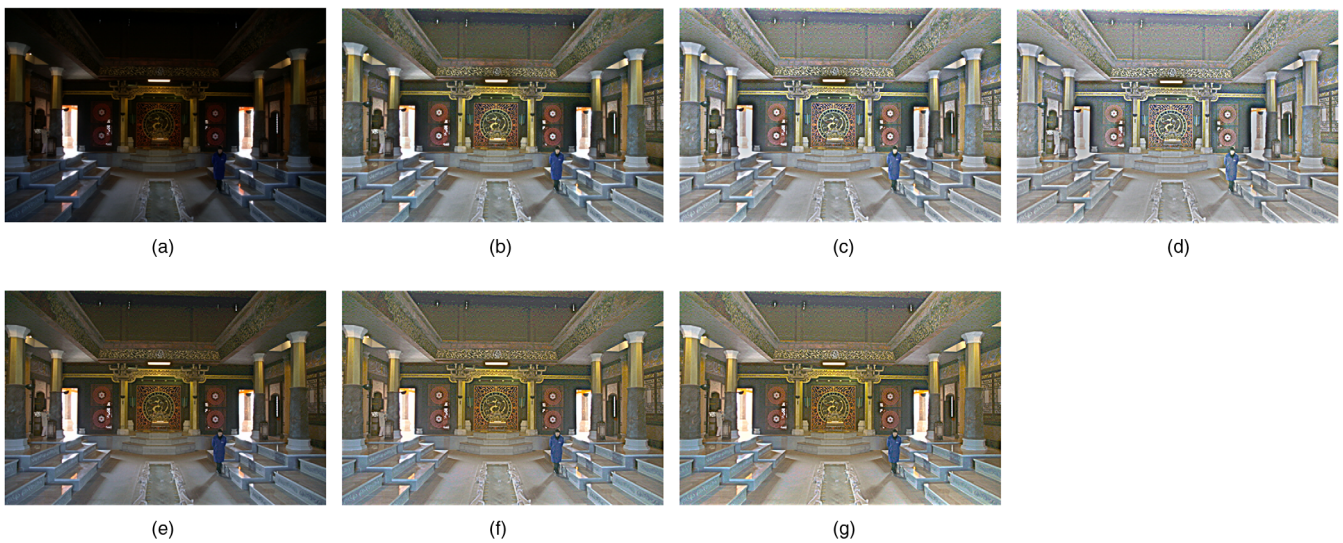

Figure 24. (a) Palace image, and images resulting from application of conventional multiscaled retinex model (b) once, (c) twice, and (d) three times, and from application of proposed method (e) once, (f) twice, and (g) three times.

objects can be recognized. Also, the colors of the landscape through the window are faded. However, in Fig. 22(d), the colors are better recovered and the noise more controlled.

Furthermore, to evaluate the stability of the proposed method as regards repeated performance, the multiscale retinex model is repeatedly applied to an input image, and Figures 23 and 24 show the images resulting when using the conventional and proposed methods, respectively. Figs. 23(b) and 23(e) show the images resulting when applying the conventional and proposed methods once. While the enhanced local contrasts are similar, halo artifacts appear on the door and lamp around in Fig. 23(b), whereas the saturation in Fig. 23(e) is more improved. However, when the conventional method is repeatedly applied, as shown in Figs. 23(c) and 23(d), the colors of the resulting images are faded and distorted. Yet, repetitive application of the proposed method does not change the color or contrast in the resulting images, as shown in Figs. 23(f) and 23(g).

Likewise, in Fig. 24, the images resulting when using the conventional method have a lower saturation than with the proposed method. In the case of repetitive application, the images resulting with the conventional method do not preserve the contrast and color, whereas the images resulting with the proposed method are unchanged.

In addition, the automatically selected parameter sets and ones hand-picked by users were compared for a qualitative evaluation. As the total number of parameters is six, controlling the algorithm manually is an arduous task. Thus, to make the process easier for the testers, the size of the large Gaussian filter was fixed at 0.8, while the range of the small and middle

Table I. Result of similarity evaluation for ten experimenters.

Experimenters	Similarity		Total similarity
	Sizes of Gaussian filter	Weights for Gaussian filters	
1	0.98	0.84	1.82
2	0.95	0.76	1.71
3	0.94	0.78	1.72
4	0.93	0.83	1.76
5	0.97	0.86	1.83
6	0.98	0.91	1.89
7	0.89	0.88	1.77
8	0.91	0.84	1.75
9	0.95	0.84	1.79
10	0.89	0.92	1.81

Gaussian filters was sampled in 2-pixel steps from 0 to 0.2. Plus, the weight sets were limited to (0.3, 0.2, 0.5), (0.3, 0.1, 0.6), and (0.2, 0.1, 0.7). Using these conditions and five test images, ten test subjects were able to find suitable parameters manually. For the selected two-parameter sets, the similarity of the weights was computed based on the large Gaussian filter. If the parameter set was the same, the similarity was 1, if the difference was 0.1, the similarity was 0.8, and if the difference was 0.2, the similarity was 0.6. In the same manner, the similarity of the size parameters decreased from 1 in steps of 0.01. Thus, if the parameter sets were the same, the total similarity was 2. Table I shows the similarity values for the ten test subjects. Overall the similarity was close to 2, indicating that the two-parameter sets selected by the proposed method and the test subjects were similar.

CONCLUSIONS

The multiscale retinex algorithm improves the local contrast and image detail using the ratio of intensity for each channel between the original image and the estimated illuminant component from Gaussian filtering. When compared with conventional methods using a gamma curve or histogram, the multiscale retinex algorithm produces good color rendition, as it considers the character of the spatially adaptive human visual system. However, its results are not stable relative to the luminance distribution of the input image. Thus, over-enhancement of the contrast and unnatural saturation can be induced.

Thus, to resolve these problems, this article proposed an adaptive multiscale retinex using Gaussian filters selected according to the intensity distribution of the input image. First, to determine the sizes and weights of the Gaussian filter set used in the multiscale retinex model, a VCM and the maximum color difference of the color patches in the Macbeth color checker are used. The visual contrast measure is obtained based on the product of the local standard deviation and the locally averaged luminance of an image. Meanwhile, to evaluate the generation of halo artifacts when large uniform regions abut to form a high-contrast edge, the maximum color difference between each color of the pixels in a patch in the Macbeth color checker and the averaged color in CIELAB standard color space is used. Moreover, to adapt the results to the input image, the standard deviation of the local luminance in the input image is used as the weight for the Gaussian filters. Considering the impact of the color difference on the generation of halo artifacts, parameters for the sizes and weights of Gaussian filters producing a higher visual contrast measure are determined.

Finally, to reduce the induced graying-out, the chroma of the resulting image from the modified multiscale retinex model is compensated by preserving the chroma ratio of the input image based on the maximum chroma values of standard sRGB color space in the lightness–chroma plane. Experimental results confirm that the proposed method is able to improve the local contrast and image details without any color distortion, while also restoring the saturation using a chroma compensation process. Future studies will investigate a method for enhancing the local contrast based on the lightness and chroma adaptation of the human visual system.

ACKNOWLEDGMENTS

This work was supported by Mid-career Researcher Program through NRF grant funded by the MEST (No. 2011-0000152).

REFERENCES

[1]B. Funt, F. Ciurea, and J. McCann, "Retinex in MATLAB™", J. Electron. Imaging **13**, 48–57 (2004).
[2]M. Ebner, *Color Constancy* (Wiley, London, 2007).
[3]T. Watanabe, Y. Kuwahara, A. Kojima, and T. Kurosawa, "An adaptive multiscale retinex algorithm realizing high color quality and high-speed processing," J. Imaging Sci. Technol. **49**, 486–497 (2005).
[4]L. Wang, T. Horiuchi, and H. Kotera, "High dynamic range image compression by fast integrated surround retinex model", J. Imaging Sci. Technol. **51**, 34–43 (2005).
[5]T. Watanabe, Y. Kuwahara, A. Kojima, and T. Kurosawa, "Improvement of color quality with modified linear multiscale retinex", Proc. SPIE **5008**, 59–69 (2003).
[6]D. Jobson, Z. Rahman, and G. Woodell, "Properties and performance of a center/surround retinex", IEEE Trans. Image Process. **6**, 451–462 (1997).
[7]Z. Rahman, D. J. Jobson, and G. A. Woodell, "Retinex processing for automatic image enhancement", J. Electron. Imaging **13**, 100–110 (2004).
[8]D. J. Jobson, Z. Rahman, and G. A. Woodell, "A multiscale retinex for bridging the gap between color images and the human observation of scenes", IEEE Trans. Image Process. **6**, 965–976 (1997).
[9]I. S. Jang, K. H. Park, and Y. H. Ha, "Color correction by estimation of dominant chromaticity in multiscaled retinex", J. Imaging Sci. Technol. **53**, 050502-1–050502-11 (2009).
[10]O. S. Kwon, Y. H. Cho, Y. T. Kim, and Y. H. Ha, "Illumination estimation based on valid pixel selection from CCD camera response", J. Imaging Sci. Technol. **49**, 308–316 (2005).
[11]J. Morovic, *Color Gamut Mapping* (Wiley, London, 2008).
[12]J. Y. Hardeberg, *Acquisition and Reproduction of Color Images* (Dissertation.com, USA, 2001).